Stabilization system for holographic recording of volume Bragg gratings using a corner cube retroreflector

Daniel B. Ott,* Ivan B. Divliansky, Marc A. SeGall, and Leonid B. Glebov

CREOL, College of Optics and Photonics, 4000 Central Florida Blvd., Orlando, Florida 32816, USA

*Corresponding author: dott@creol.ucf.edu

Received 29 October 2013; revised 14 January 2014; accepted 15 January 2014;
posted 16 January 2014 (Doc. ID 200320); published 12 February 2014

Volume Bragg gratings serve an important role in laser development as devices that are able to manipulate both the wavelength and angular spectrum of light. A common method for producing gratings is holographic recording of a two collimated beam interference pattern in a photosensitive material. This process requires stability of the recording system at a level of a fraction of the recording wavelength. A new method for measuring and stabilizing the phase of the recording beams is presented that is extremely flexible and simple to integrate into an existing holographic recording setup and independent of the type of recording media. It is shown that the presented method increases visibility of an interference pattern and for photo-thermo-refractive glass enables enhancement of the spatial refractive index modulation. The use of this technique allows for longer recording times that can lead to the use of expanded recording beams for large aperture gratings.

OCIS codes: (120.5050) Phase measurement; (120.7280) Vibration analysis; (090.7330) Volume gratings; (050.1950) Diffraction gratings; (120.3180) Interferometry; (090.0090) Holography.

http://dx.doi.org/10.1364/AO.53.001039

1. Introduction

Volume Bragg gratings (VBGs) are a widely used optical component for applications such as spectral and angular shaping, communications, and sensing due to their ability to diffract into a single order with high efficiency when the Bragg condition is met. VBGs are created by producing a spatially varying sinusoidal pattern of the refractive index inside a photosensitive medium and are typically produced using holographic exposure, lithography, phase masks, or point by point inscription [1–3]. These methods apply most readily to VBGs written into optical fibers. For VBGs in a bulk medium with apertures exceeding several millimeters, holographic recording of a two-beam interference pattern (Fig. 1) is the most suitable approach. This method can be used to create both reflecting and transmitting VBGs of different spatial frequencies by adjusting the recording angle of interference. To achieve high-quality volume gratings with high efficiency and periods as low as 200 nm, it is necessary to be able to generate an interference pattern with high-fringe visibility and a uniform period throughout the volume of the medium together. These conditions provide a constant resonance condition combined with high-contrast refractive index modulation (RIM). As an example, for gratings being designed as output couplers for laser systems, it is usually necessary to achieve very specific spectral widths and angular selectivity in addition to precise diffraction efficiency, making it critical to have exact control over the RIM [4]. The primary detriment to obtaining consistent fringe visibility, and therefore high-quality VBGs, is shifting of the interference fringes during the recording process. Such fringe movement could be due to vibrations of beam delivery optics or the

1559-128X/14/061039-08$15.00/0

sample, as well as localized changes in the relative density of air along the paths of the recording beams.

By measuring and controlling the relative phases in the recording beams, high-visibility fringes can be maintained throughout the recording. The resulting VBG will have a consistent index modulation with efficient use of the material's dynamic range. To control the phase of the interference pattern, a number of different methods have been proposed [5–10]. One of the most elegant and direct solutions is the use of the dynamically formed grating to diffract a portion of each recording beam into the other recording beam generating an interference pattern [7]. This process of dynamic wave-mixing allows for direct monitoring of the relative shift of the interference pattern and the current grating structure. The drawbacks of this method relate to the restrictions that it places on the recording media. Using the dynamic grating formation requires that the recording medium has low absorption at the recording wavelength and that it does not introduce significant distortions into the beams. Most importantly, the material must also form a weak grating during the recording process. This may not always be the case when a latent image is formed and further development is necessary, or when the parameters of the recording substrate are such that a useful diffraction efficiency cannot be achieved. So, while the use of dynamic wave-mixing is applicable to some holographic recording setups, it lacks the flexibility necessary for recording gratings in a variety of materials. The use of an auxiliary reference grating to wave-mix the recording beams can also generate an appropriate feedback signal. This can be achieved by placing a reflection or transmission grating next to or behind the recording medium [6,7,10]. A portion of the recording beams is diffracted by the reference grating and is used for phase stabilization. The rest of the recording beam is used to expose the photosensitive material to create the desired grating. Such systems remove any restrictions caused by the properties of the recording media. However, they also present a major limitation in that a reference diffractive element can only be used for a particular angle of incidence at the recording wavelength. This limits the utility of such stabilization systems to a particular recording angle corresponding to the resonance condition of the diffractive element thus being useful for creating only a specific grating period. To record a grating of a different spatial period requires a new reference grating to be fabricated or purchased. Therefore, requiring a reference grating would nearly double the time requirement for producing a particular grating when reference gratings cannot be reused. The ability to use the same phase control system for any grating period is a critical requirement for any universal recording system for fabrication of gratings with different parameters. To address the need for a versatile phase stabilization system, we propose a new, flexible phase measurement technique that can be applied to most common holographic recording setups. In our approach, the reference grating is substituted with a corner cube retroreflector and the feedback signal is monitored at a different location. These improvements yield a new interferometer that is both independent of the recording medium and able to be used to control the relative phase of a two-beam interference pattern with any spatial period. The system that we propose results in an effective, versatile, and simple to align system for measuring and controlling the relative phase in a holographic recording.

2. Tolerances for Phase Stabilization

Before describing the method for stabilizing interference fringes, it is important to determine the effect of an uncontrolled fringe pattern. When using two-beam interference to record a grating (Fig. 1), the resulting spatial RIM of the grating is directly proportional to the two-beam interference intensity pattern when operating within the linear region of the material photosensitivity curve [11]. This interference pattern is given by Eq. (1)

$$I(x) = I_1 + I_2 + 2\sqrt{I_1 I_2}\cos(2kx\,\sin\theta + \varphi), \qquad (1)$$

where I_1 and I_2 represent the irradiance of each recording beam, and the resulting index modulation profile is proportional to the cosine with a period determined by the wave vector (k) of the recording beam and the angle of interference θ. The term φ is the relative shift in phase between the two recording beams. Modification of any of the arguments in the cosine of Eq. (1) will result in a shifting fringe pattern. For the current analysis, the wave vector of the recording laser is held constant and the angle of interference is assumed stable at the arc second level such that no significant change in period occurs. In our setup, this stability has been confirmed experimentally by measuring the angle stability of

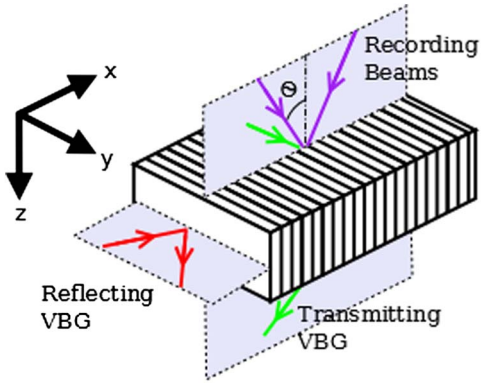

Fig. 1. General recording and readout for a VBG. Rays marked purple indicate the recording beams that generate the interference pattern at a wavelength within the photosensitivity spectrum of the medium. After recording and development, the grating can be used as a transmitting grating for beams at a different wavelength marked as green or at yet another wavelength the grating can be used as a reflecting grating for beams indicated by red.

the recording mirrors by forming a Sagnac interferometer and monitoring the shifts of fringes. Practically speaking, this level of stability in angle is not difficult to achieve with commercially available optical mounts and a vibration-isolated table. The most significant effect on the interference pattern comes from changes in φ, primarily due to vibrations in the recording setup and air fluctuations. This results in a shifting of the relative phases between the recording beams as a function of time. The recorded interference pattern in this case is given by Eq. (2)

$$I_{\text{final}}(x) = I_1 + I_2 + \int_0^T 2\sqrt{I_1 I_2}\cos(2kx\,\sin\theta + \varphi(t))\mathrm{d}t. \quad (2)$$

The effect of randomly varying phase difference about a mean value can also be calculated to determine a tolerance to phase noise allowable in a recording system. For this calculation, we assume a randomly varying phase difference described by a Gaussian probability density function that will allow the effect on the fringe pattern to be described by a single parameter relating to the variance of the phase fluctuations. The probability density function for a randomly distributed phase variation is shown in Eq. (3)

$$W(\varphi) = \frac{1}{\sqrt{2\pi}\sigma} e^{\left(\frac{-\varphi^2}{2\sigma^2}\right)}, \quad (3)$$

where σ is the root mean square error (RMSE) about the average phase value. The interference pattern can then be described by the integral in Eq. (4)

$$I_{\text{final}}(x) = I_1 + I_2 + \int_{-\infty}^{\infty} W(\varphi)\cdot 2\sqrt{I_1 I_2}\cos(2kx\sin\theta + \varphi)\mathrm{d}\varphi. \quad (4)$$

The fringe visibility of the resulting interference pattern (V) is the metric that will be used to determine the quality of the recorded grating. This value is a normalized indicator for the amount of the maximum possible index change that can be achieved

$$V = \frac{I_{\max} - I_{\min}}{I_{\max} + I_{\min}}. \quad (5)$$

Equation (4) was integrated numerically for a number of σ values to determine the effect of fringe shift on the visibility. The results of fringe visibility deterioration are shown in Fig. 2 as a function of phase variations σ measured in units of fractions of the recording wavelength. The value of σ in radians can be determined from the x axis value by multiplying by 2π. As the amplitude of the phase variations increases, the fringe visibility starts to decrease, resulting in a weakened RIM. For high values of σ beyond 0.5 waves, the fringe pattern will be effectively washed out because the phase during recording with cover a full 2π range. Therefore, practical systems for holographic recording are most likely operating in the range shown in Fig. 2. The inset in Fig. 2 shows the region of minimal phase fluctuations in that we plan to operate using phase stabilization. In this region, the decrease of visibility is relatively slow. A tolerance of fluctuation amplitude less than 5% of a recording wavelength will guarantee fringe visibility >95% of the optimum value.

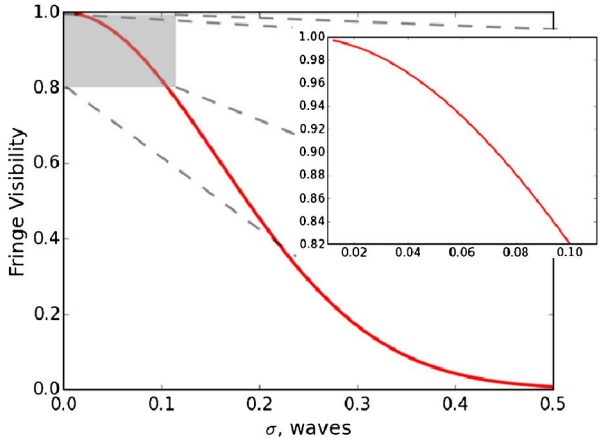

Fig. 2. Dependence of interference pattern visibility on phase fluctuations during recording. Phase variation σ is shown as a fraction of the recording wavelength. Inset shows fringe visibility for small phase fluctuations.

3. Setup and Characterization

The phase stabilization techniques described in prior art all rely on a feedback loop consisting of a phase measurement method, a phase shifting device, and some signal processing. The main emphasis in the current work is on the development of a sensitive and robust method for measuring phase fluctuations. The phase shifting device is most commonly a piezoelectric transducer (PZT) placed on a turning mirror that allows small shifts in path length to be introduced into one of the recording arms. A PZT is used in this system, but any phase shifting device with an appropriate response time is equally well suited. The performance of any stabilization system can be significantly improved by using appropriate signal processing, and there is a wealth of information regarding various methods for processing the feedback signal. These methods have not been implemented in the current system and are a matter of further improving the system that is presented here. This can lead to better frequency response and insensitivity to changes in incident power levels but, as we will demonstrate, are not critical for the effective stabilization of our recording setup. The phase measurement technique has the greatest consequences in terms of the recording setup and will be the focus of the technique that we demonstrate in this paper.

The entire recording setup is shown in Fig. 3. At the recording plane, a small portion of the recording beam is used to measure the relative phases

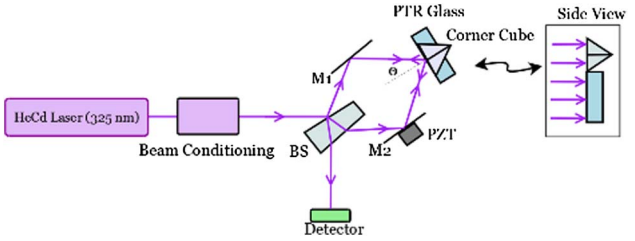

Fig. 3. VBG recording setup showing the paths of the recording/probe beam. BS, beam splitter; M1 and M2, mirrors; PZT, piezoelectric transducer. The side view shows how the beam is split between a recording portion and a probe portion for measuring phase.

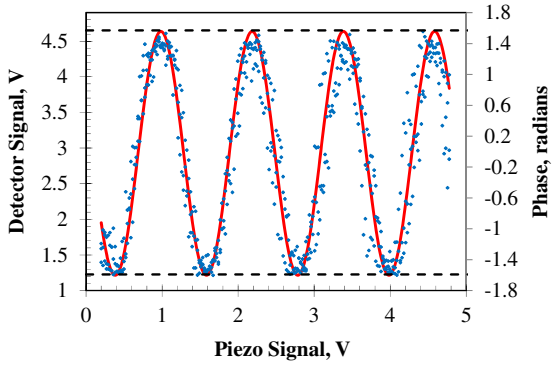

Fig. 4. Phase shift between recording beams measured by the detector in Fig. 3 as a function of voltage applied to the PZT that causes a position change of the recording mirror, M2. The red line shows a sinusoidal fit to the experimental data in blue dots.

of the beams while the rest is used to expose the photosensitive material. The portion of the beam used for phase measurement will be called the probe beam. The phase measurement is achieved through a corner cube retroreflector that is placed above the sample. The probe and recording portions of the beam trace along collinear paths to reach the recording plane and the probe beam is then reflected back along this path to double the relative phase deviations that are incurred. At the detector plane, the back-reflected probe light forms an interference pattern and the corner cube is adjusted in position to achieve overlap of the two collinear probe beams so that the entire probe beam diameter gives a zero-fringe interference pattern. One of the primary benefits of this method is that the precision of this alignment can be very coarse. The retroreflector guarantees angular alignment and beam overlap can be achieved without the use of precision stages.

As the relative phases of the paths change, the irradiance at the detector will vary as Eq. (1) with $\theta = 0$. By using a retroreflector, the system can be easily moved and realigned for recording gratings of different period and arbitrary grating tilt angles. The detector signal is used as feedback and a PZT is placed beneath one of the mirrors (M2 in Fig. 3) to correct for measured phase fluctuations by maintaining a constant detector signal. The feedback control is extremely simple and, in systems control language, consists of only a proportional gain. Again, introducing other signal processing techniques can be used to improve the performance of the system, but for what is demonstrated here only a simple control system is necessary.

The phase difference between the recording beams can be extracted from the measured variations in the detector voltage. In order to determine the conversion factor between the detector's voltage and the probe beam phase difference, a calibration of the system was performed prior to any measurement of phase. The calibration was accomplished by driving the PZT with a ramp function to generate a sinusoidal variation in the detector voltage with a period corresponding to a phase difference in the probe beams of 2π, as shown in Fig. 4. By fitting a sinusoid to this curve, a conversion function was calculated to convert a detector voltage to a phase difference between the beams.

While the shifting of the phase of the two recording beams is important to the stability of the setup and has many components that can contribute to errors, the displacement of the sample must not be ignored. The sample has six degrees of freedom, but primarily tilt about the y axis and displacement in the x axis of Fig. 1 can contribute to errors in the recording. The errors of tilt only affect the recording substantially in the shift that they induce in various parts of the grating relative to other parts. Therefore, the displacement in x, which will be referred to as lateral shift, is a critical motion to control and the question of whether or not the proposed system is sensitive to these motions must be answered. To the best of our knowledge, no studies have been conducted that relate to the sensitivity of a phase stabilization system to lateral motion. Since this motion is as equally detrimental as phase changes that occur in the delivery path, such a study is extremely important.

The sensitivity to lateral shift of the corner cube retroreflector used in Fig. 3 will be compared to the most common method of phase stabilization [8] that uses a transmission reference grating. Recently, reflection gratings have been shown to produce a phase shift under lateral displacement giving promise to the idea that a phase stabilization system based on transmission gratings is sensitive to the lateral shift of the recording media [12]. While counterintuitive, a shift of a transmitting or surface reflection grating by one period will shift the relative phase of the transmitted and diffracted orders by 2π. Therefore, there is a one-to-one correspondence between the lateral shift in the measurement device (measured in number of wavelengths) and the shift of the interference pattern that is monitored to measure phase. This makes phase control systems using a grating able to measure and correct for lateral shifts.

To show that a retroreflector is also sensitive to these shifts, the nature of the optical path to and

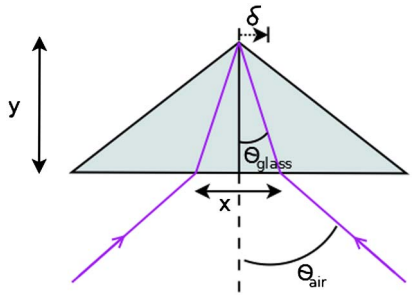

Fig. 5. Diagram of a retroreflector in a phase stabilization system with designation of variables for calculating lateral sensitivity.

from the retroreflector must be considered. The optical path encountered by a ray that has traveled from a particular phase plane, reflected off of any part of the retroreflector and back to that plane, is equal to twice the distance from the initial phase plane to the optical center of the corner cube [13]. Therefore, it is possible to model optical path length in an interferometer by geometrically drawing a line from a reference point in the beam path to the optical center of the corner cube. Since this system deals with measuring relative lateral shifts, the location of this optical center is not important and can be considered to be located at the corner cube vertex [14]. With this understanding, it is intuitive from Fig. 5 that a shift of δ will cause a relative phase shift between two incident beams. This is because the optical path for one beam will shorten, while the other will lengthen. Mathematically this takes the form

$$\text{OPD} = 2n_0\left(\sqrt{(x+\delta)^2+y^2} - \sqrt{(x-\delta)^2+y^2}\right),$$
$$\text{where } y = x/\tan\,\theta_{\text{glass}}, \tag{6}$$

OPD is the optical path difference, θ_{glass} is the angle within the glass, n_0 is the refractive index of the corner cube, and the planes of equal phase are considered the entrance of the beams into the corner cube for simplicity. Assuming the square of the displacement is negligible, Eq. (6) can be simplified to the result in Eq. (7)

$$\text{OPD} = 4n_0\delta\,\sin\,\theta_{\text{glass}}. \tag{7}$$

The period of the grating that is recorded is given by $\lambda_{\text{rec}}/(2n_{0\text{–rec}}\,\sin\,\theta_{\text{glass-rec}})$. Due to the invariance of the product of $n_0\,\sin\,\theta$ by Snell's law, and the use of the same beam as the probe and for recording, the medium of the retroreflector is insignificant. Therefore, if the retroreflector shifts by one grating period, the measured OPD will be twice the period. This corresponds exactly with the results we expect from this system because it is designed to measure fringe shifts caused by phase variations before the recording plane in a double-pass configuration.

Experimental verification of the sensitivity to lateral motion was conducted to confirm the accuracy of our approximations. The experimental setups for comparing the sensitivity of the retroreflector to the sensitivity of a transmitting VBG are shown in Fig. 6. Along with verifying the presence of lateral sensitivity in a retroreflector, experimental verification of the lateral sensitivity of a transmitting VBG is important since all previous discussion of grating sensitivity to lateral motion was conducted using thin gratings.

In the setups of Fig. 6, the PZT was oriented such that it could induce lateral shifts of the two phase measurement devices. Both interferometers were aligned to measure the interference of a He–Ne laser operating at 633 nm and incident on the devices at approximately 13.5°. The transmitting VBG is designed to diffract light at this angle with approximately 50% diffraction efficiency. When each incident beam is aligned to the Bragg angle and they overlap spatially, the diffracted beam of one arm and the transmitted beam of the other arm of the interferometer will be collinear. The detected intensity will be a measure of the relative phase difference between the two arms. To observe the sensitivity to lateral motion of each of the setups, the PZT was ramped through a voltage range and the intensity

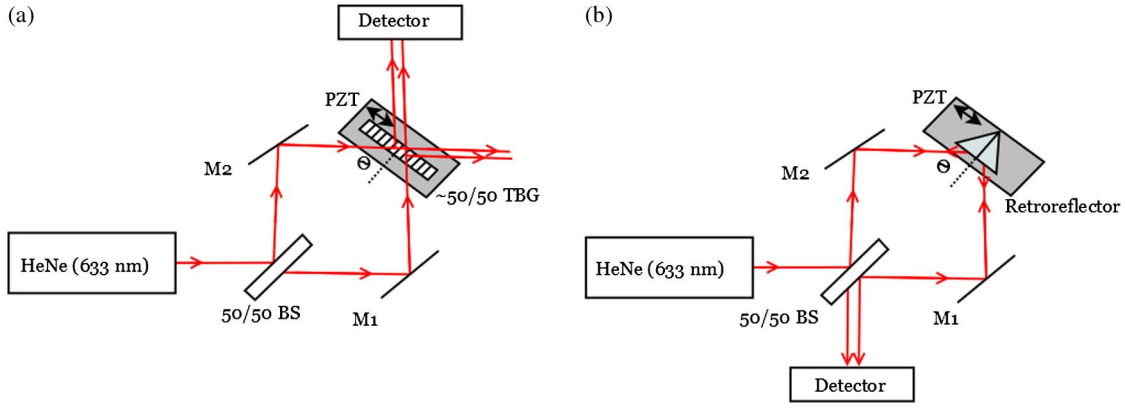

Fig. 6. Experimental setup to study the sensitivity of phase measurement to lateral displacement for (A) a transmitting VBG and for (B) a corner cube retroreflector. The PZT is used to shift the respective measurement device. The effect of lateral shift on the signal measured at the detector is monitored.

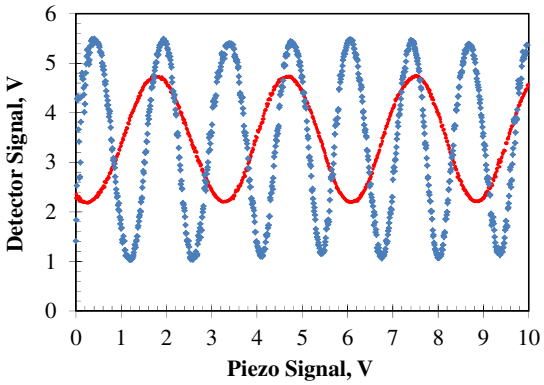

Fig. 7. Dependence of signals measured by the detectors in Figs. 6(A) and 6(B) on a signal applied to the PZT controlling lateral displacement of a TBG (red) and a retroreflector (blue). The difference in the visibility of these fringes is not inherent to the measurement device but is determined by alignment of components.

change at the detection plane was monitored. The two signals that were received are shown in Fig. 7. Both methods result in periodical signals at the detectors caused by phase incursion between the interfering beams and, therefore, demonstrate measureable sensitivity to lateral shifts induced by the PZT. The most important feature to note is the roughly twice higher frequency of the oscillations in the retroreflector signal, as expected by theory. The difference between the frequencies of each signal is not exactly a factor of two. This discrepancy is simply due to not precisely controlling the direction of the PZT motion to be exactly orthogonal to the axis of interference.

Another important feature is the higher visibility of the fringes produced by the retroreflector. While this increased visibility is not necessarily related to a difference between the systems, it does highlight the ease of alignment afforded by the use of the retroreflector. A reference grating system requires that the grating be aligned to the interfering beams in tip about the y axis and roll about the z axis and for small beams, displacement about the z axis to obtain good beam overlap. In a system that uses a dynamically formed grating to measure phase, this alignment is automatic. For a stabilization system using a reference grating, this alignment requires a high level of accuracy and can be difficult to obtain high visibility of the phase measurement. Despite these differences it is clearly shown that both methods have sensitivity to lateral motion and the relative sensitivity confirms the results in Eq. (7), making both methods equally suitable for correcting these detrimental motions in a holographic recording.

4. Effect of Phase Stabilization on VBG Performance

It is important to note that the performance of a phase stabilization system cannot be completely evaluated by detecting the feedback signal with the system operating in an open feedback loop and then closing the loop and comparing the relative amplitudes of fluctuations between the stabilized and unstabilized system. While this would demonstrate the effectiveness of the feedback system, it does not directly show the effect that this has on the quality of the VBG recording. If phase stabilization results in no change in the grating performance, the system is either measuring incorrectly or phase fluctuations are not responsible for quality of recording. Based on the analysis of the effects of phase fluctuations presented in Section 2, the primary effect of an unstabilized system is to reduce the RIM. Therefore, by demonstrating an improvement of a grating's RIM we can conclude that phase fluctuations were deteriorating the RIM depth and that phase stabilization was successful in controlling these fluctuations. This experiment was conducted using the setup depicted in Fig. 3 to record reflecting VBGs with a resonant wavelength of 978 nm and the time for each recording was 22 min. The recording material for these experiments is photo-thermo-refractive glass, which has proven in recent years to be an excellent material for recording high-quality VBGs [15,16]. This material is photosensitive to UV radiation and develops a permanent RIM after thermal development.

From these recordings, an increased RIM due to increased fringe visibility in the phase-stabilized recordings is expected to be observed. In a reflecting VBG with high-diffraction efficiency, an increased RIM will correspond to a higher bandwidth. The RIM can be calculated by matching measured spectral response to those calculated by coupled wave theory using measured parameters for thickness and resonant wavelength [17,18]. After exposure and development, the recorded gratings were cut to a thickness of 3.75 mm and transmission spectra were measured using a tunable laser. The transmission spectrum of each grating was used to determine the RIM induced in each recording [18].

The first grating was recorded with no stabilization present. Figure 8(A) shows the phase difference calculated from the measured feedback signal before and during the recording, using Fig. 4 for conversion. The relative phase of the beams has both high-frequency noise and slow oscillations. These oscillations are the result of phase drift in one direction because the detector is measuring the sinusoid of a phase term and there is a 2π phase ambiguity.

The phase during recording [Fig. 8(A)] was analyzed by using Eq. (2) to determine the expected fringe visibility that can be achieved by recording in this condition. The measured data predicts that the RIM will be 76% $\pm$5% of a perfect recording with no phase shifts. Uncertainty in this measurement is due to changes in the average intensity in the recording beam and is evident only when observing a change in the inflection points of the signal in the region near $\pm\pi/2$. The measured transmission spectrum is shown in Fig. 9(A) together with the theoretical spectrum that provides the same spectral

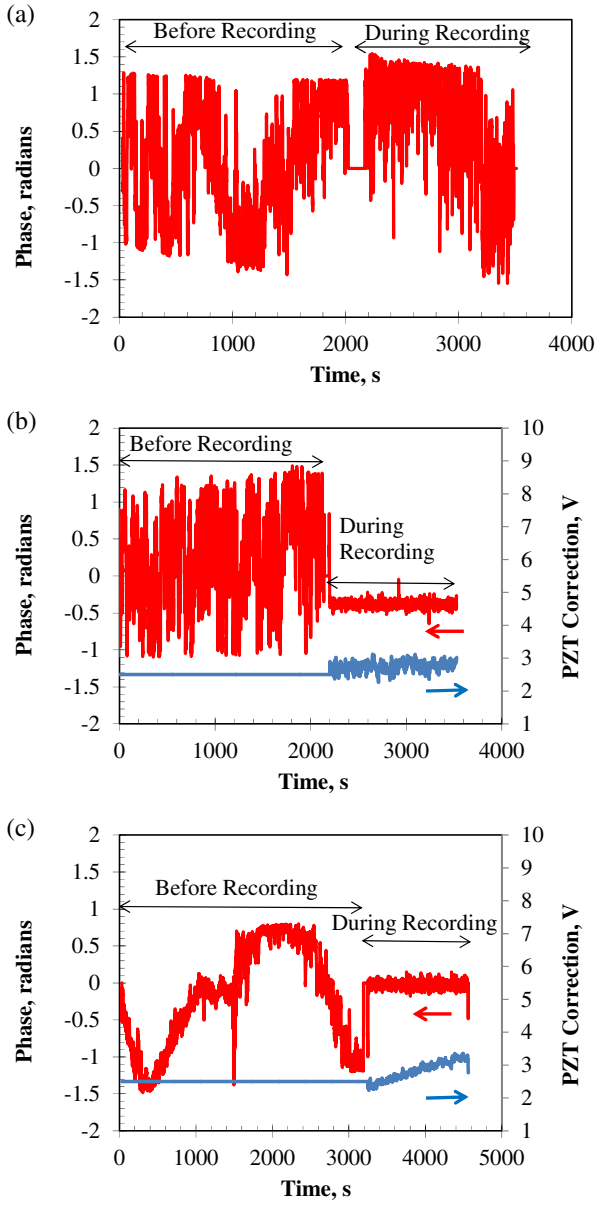

Fig. 8. Phase fluctuations at a detector depicted in Fig. 3 for the recording of gratings (A) without and (B) and (C) with phase stabilization. The relative phase of the recording beams with no stabilization shows both high-frequency noise and long-term variations. The relative phase of the recording beams with stabilization shows dramatic decrease of both high-frequency noise and long-term variations. The correction voltage applied to the PZT is shown in blue.

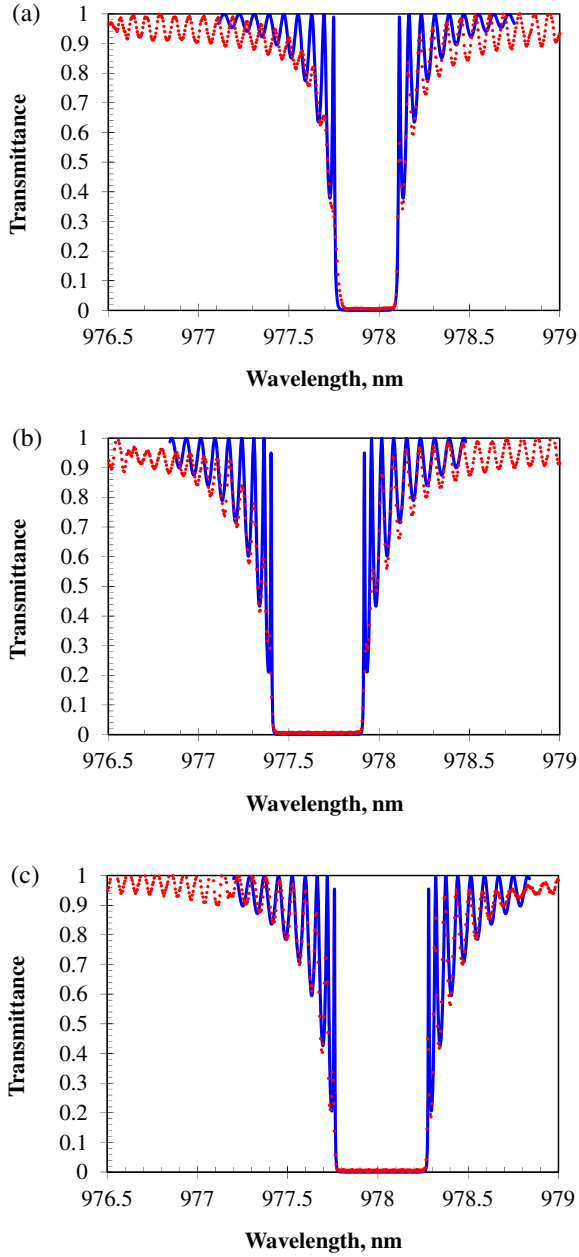

Fig. 9. Transmission spectra of 3.75 mm thick gratings with the same periods recorded (A) without and (B) and (C) with phase stabilization. The FWHM bandwidths are 430, 660, and 670 pm for plots (A), (B), and (C), respectively. Red, experiment; blue, coupled wave theory simulation.

width. The RIM was calculated by matching the measured spectrum to a theoretical spectrum. An excellent agreement of the shapes of both spectra can be seen in the figure. For a 3.75 mm thick RBG with resonant wavelength of 978 nm, a 430 pm bandwidth corresponds to a RIM of 490 ppm.

A second RBG was recorded using the same parameters. During the recording process, the PZT was used to maintain a constant relative phase of the recording beams. Figure 8(B) shows the phase variations before and during recording. Monitoring the phase variations before recording allows phase noise present in the recording environment to be determined. The remaining noise during stabilization has a RMSE of 0.0052λ and the expected visibility of this recording is 99.8%. The signal sent to the PZT during the recording is shown on the same plot to demonstrate how it was used to counteract the phase noise. The spectral response of this grating was also measured and fit to theory in Fig. 9(B). At a thickness of 3.75 mm, the bandwidth of 660 pm corresponds to a RIM of 740 ppm.

The demonstration of improvement of RIM was significant but does not rule out all possible noise sources that deteriorate the recording conditions. For example, the grating shown in Fig. 9(B) did not undergo a long-term phase drift as was present in the unstabilized case. To address these concerns, a third reflecting VBG was recorded when the environmental phase variation [Fig. 8(C)] was demonstrating different behavior. This environment differs from the environment in Fig. 8(B) in that there is a slow, long-term drift and the amplitude of the high-frequency phase noise is much lower. These two different scenarios are evidence of the various operating conditions that can be encountered in a typical laboratory environment. When recording in this environment, the relative phase difference between the recording beams was again significantly decreased by the use of phase stabilization and the RMSE noise is 0.0057λ. The predicted visibility from this phase is 99.7%. The correction voltage applied to the PZT shows a linear drift during the recording, indicating that it is working against the linear drift in the environment as expected. The measured transmission spectrum in Fig. 9(C), at a thickness of 3.75 mm, gave a bandwidth of 670 pm corresponding to a RIM of 750 ppm. This value matches well with that of the grating in Fig. 9(B), confirming proper measurement of relative phase and effective correction. Thus, the grating recorded without phase stabilization has a RIM that is 66% of the RIM in the grating recorded with stabilization. This deviates from the calculation that predicts 76% but is of the right general scale given the uncertainty in the measurement and typical homogeneity of about 5% for RIM. The use of this phase stabilization system is shown to correct the phase to a level where consistent high-visibility fringes can be recorded over long exposure times. The increase in fringe visibility manifests itself as a broader reflection bandwidth in the experiments presented here and we have demonstrated an increase of RIM by 50%. Using this system will allow longer recording times, meaning that lower irradiance beams can be used for recording larger aperture gratings.

5. Conclusion

For holographic recordings of volume Bragg gratings with fringe visibility exceeding 95%, random noise variations must be maintained below 0.05λ. The active stabilization system proposed here produces phase stabilization well below this level by using a corner cube retroreflector to sample the recording beams and measure the relative phase difference. This system is versatile in the sense that it can be used to stabilize an interference pattern with any spatial period. The lateral sensitivity of the retroreflector system was verified experimentally to show that it is comparable to other common methods of phase stabilization. The effectiveness of the system was verified by recording reflecting volume Bragg gratings both with and without phase stabilization. By reducing phase noise during recording, the visibility of the interference pattern was improved, leading to an increase of the RIM in the final VBG. An increase in the RIM by 50% was demonstrated in PTR reflecting Bragg gratings using this phase stabilization system. The system can be used to ensure fringe visibility of >99% in a holographic recording, independent of the recording media and is applicable to any grating period or tilt.

This work was funded by HEL/JTO and ARO (contract W911NF-10-1-0441).

References

1. R. R. Syms, *Practical Volume Holography* (Clarendon, 1990), pp. 21–26.
2. K. O. Hill, B. Malo, F. Bilodeau, D. C. Johnson, and J. Albert, "Bragg gratings fabricated in monomode by UV exposure through a phase mask photosensitive optical fiber," Appl. Phys. Lett. **62**, 1035–1037 (1993).
3. A. Martinez, I. Y. Khrushchev, and I. Bennion, "Thermal properties of fibre Bragg gratings inscribed point-by-point by infrared femtosecond laser," Electron. Lett. **41**, 176–178 (2005).
4. G. Venus, A. Sevian, V. Smirnov, and L. Glebov, "Stable coherent coupling of laser diodes by a volume Bragg grating in photothermorefractive glass," Opt. Lett. **31**, 1453–1455 (2006).
5. D. B. Neumann and H. W. Rose, "Improvement of recorded holographic fringes by feedback control," Appl. Opt. **6**, 1097–1104 (1967).
6. D. MacQuigg, "Hologram fringe stabilization method," Appl. Opt. **16**, 291–292 (1977).
7. A. A. Kamshilin, J. Frejlich, and L. H. Cescato, "Photorefractive crystals for the stabilization of the holographic setup," Appl. Opt. **25**, 2375–2381 (1986).
8. C. C. Guest and T. K. Gaylord, "Phase stabilization system for holographic optical data processing," Appl. Opt. **24**, 2140–2144 (1985).
9. J. Muhs, P. Leilabady, and M. Corke, "Fiber-optic holography employing multiple beam fringe stabilization and object/reference beam intensity variability," Appl. Opt. **27**, 3723–3727 (1988).
10. L. De Sio, R. Caputo, A. De Luca, A. Veltri, C. Umeton, and A. V. Sukhov, "In situ optical control and stabilization of the curing process of holographic gratings with a nematic film-polymer-slice sequence structure," Appl. Opt. **45**, 3721–3727 (2006).
11. J. W. Goodman, *Introduction to Fourier Optics* (McGraw-Hill, 1996), pp. 297–298.
12. S. Wise, V. Quetschke, A. Deshpande, G. Mueller, D. Reitze, D. Tanner, B. Whiting, Y. Chen, A. Tünnermann, E. Kley, and T. Clausnitzer, "Phase effects in the diffraction of light: beyond the grating equation," Phys. Rev. Lett. **95**, 013901 (2005).
13. C. Rothleitner and O. Francis, "On the influence of the rotation of a corner cube reflector in absolute gravimetry," Metrologia **47**, 567–574 (2010).
14. G. M. Kuan and S. J. Moser, "Sensitivity of optical metrology calibration to measured corner cube retroreflector parameters for the space interferometry mission," Proc. SPIE **4852**, 795–802 (2013).
15. L. Glebov, V. Smirnov, C. Stickley, and I. Ciapurin, "New approach to robust optics for HEL systems," Proc. SPIE **4724**, 101–109 (2002).
16. L. Glebov, "Volume holographic elements in a photo-thermo-refractive glass," J. Hologr. Speckle **5**, 77–84 (2009).
17. H. Kogelnik, "Coupled wave theory for thick hologram grating," Bell Syst. Tech. J. **48**, 2909–2947 (1969).
18. I. Ciapurin, D. Drachenberg, V. Smirnov, G. Venus, and B. Glebov, "Modeling of phase volume diffractive gratings, part 2: reflecting sinusoidal uniform gratings, Bragg mirrors," Opt. Eng. **51**, 058001 (2012).